

Static and dynamic conductivity of amorphous nanogranulated composites

© I.V. Antonets, R.I. Korolev, L.N. Kotov

Syktyvkar State University,

Syktyvkar, Russia

E-mail: aiv@mail.ru

Received April 30, 2024

Revised October 28, 2024

Accepted October 30, 2024

The results of an experimental study of the static and dynamic conductivities of amorphous nanogranulated composites $(\text{CoFeB})_x + (\text{SiO}_2)_{1-x}$, $27.38 \leq x \leq 84.14$ at.% 493–862 nm thick, deposited on a lavsan substrate 0.02 mm thick, are presented. The spectra of the impedance modulus and phase angle in the range of 50 kHz–15 MHz are obtained. The frequency dependences of dynamic conductivity in the ranges of 50 kHz–15 MHz and 8–12 GHz, as well as the ratio of dynamic to static conductivity on the ferromagnetic alloy content at various frequencies are given. It is shown that the dynamic conductivity up to the percolation threshold can exceed the static one by more than 2–4 orders of magnitude. The influence of the structural characteristics and composition on the conductive properties of the films is determined.

Keywords: composite films, impedance, reflection coefficient.

DOI: 10.61011/PSS.2024.12.60169.6373PA

1. Introduction

Amorphous nanogranular composites exert unique anisotropic, conducting and structural properties [1–4], and the opportunities to control these properties at the expense of nanotechnology development and structure modification are far-reaching in development of new small-scale microwave devices in the modern optoelectronics, sensorics, personalized medicine, microwave systems of information transmission [5–10].

2. Experiment

Composite films are made by method of ion-beam deposition in the argon atmosphere at low vacuum 10^{-5} Torr in the Voronezh State Technical University. The elemental analysis was carried out using an energy-dispersive attachment to a scanning electron microscope Axia ChemiSEM ThermoFisher (Czech Republic). Static conductivity on direct current were measured in a two-wire circuit, using a digital multimeter HP Agilent Keysight 34401A. The film with dimensions of 7×3 mm was attached by a lavsan substrate to a fabric-based laminate foiled plate (holder) with a 5 mm long dielectric gap. A current-conducting site was applied on the ferromagnetic layer of the film with the help of a silver paste, which was closed with a copper foil on the fabric-based laminate. As a result, an area was formed for a change with the size of 5×3 mm in the gap between the current-conducting paste. The static conductivity was calculated using the following formula

$$\sigma_0 = \frac{l}{r_0 \cdot S}, \quad (1)$$

where S — cross section of the conducting layer of the film, l — film length between the measuring pins, r_0 — electrical resistance on direct current. Medium and high frequency dynamic conductivity (50 kHz–15 MHz) was assessed using the measurements of impedance module and phase angle with the help of a immitance meter E7-29 with UP-5 device connected thereto. The measurements were made in automatic mode with a frequency pitch of 100 kHz and were recorded in the computer memory. Dynamic microwave conductivity in the frequency range 8–12 GHz was calculated using the measurements of the reflection coefficient in a rectangular waveguide [11].

3. Results

Previously we investigated the amorphous nanogranular composites with composition $(\text{Co}_{41}\text{Fe}_{39}\text{B}_{20})_x(\text{SiO}_2)_{1-x}$ [11,12]. In these papers the conducting properties of the films are first of all due to the content of 20% boron half-metal in the ferromagnetic alloy composition. In AFM images the point nanoscale areas of conductivity were localized only at the tops of the largest particles of the ferromagnetic alloy. Therefore, the specific conductivity varied from 10^{-8} to 10^{-4} S/m. In the specimens studied in this paper, the boron content was 3–5%, which made it possible to increase the range of conductivity variation, from 10^{-2} to 10^5 S/m. Besides, the studies presented in [11,12], were carried out mainly with the contents of ferromagnetic alloy before the percolation threshold (32.79–52.00 at.%). In this paper the range of metal phase concentrations of the studied specimens made it possible to decide on the conducting properties both prior

to the percolation threshold (from 27.38 at.%), inside the percolation region, and significantly beyond the percolation threshold (up to 84.14 at.%). The main characteristics of composite films are presented in the table.

Frequency spectra of impedance module $|Z|$ and phase angle θ were obtained in the range of 50 kHz–15 MHz. Active component of electrical resistance —

$$r = |Z| \cos \theta. \quad (2)$$

Using geometric dimensions of the specimen and the distance between the contacts, the dynamic conductivity was found:

$$\sigma = \frac{l}{|Z| \cos \theta \cdot S}. \quad (3)$$

In the frequency range of 8–12 GHz the dynamic conductivity σ according to the measured reflection coefficient of the specimens R was assessed with the help of the logic for calculation of structural and conducting characteristic of amorphous nanogranular composites [13], with the use of the closed chain mechanism in the model of intragranular currents [13,14]:

$$\sigma = \frac{2}{Z_0 d_{\text{eff}} (1/\sqrt{R} - 1)}, \quad (4)$$

where Z_0 — impedance of free space, d_{eff} — effective thickness of the composite film layer, which accounts for the main part of the ferromagnetic alloy made of conducting granules, i.e. [14]:

$$d_{\text{eff}} = d \cdot \frac{x, \text{ at.\%}}{100\%}, \quad (5)$$

x — content of ferromagnetic alloy in at.%.

Figure 1 provides the experimentally measured dependences of the impedance module (a) and the calculated dynamic conductivity (b) in the frequency range of 50 kHz–15 MHz.

From Figure 1 one can see that the significant changes of the impedance module and dynamic conductivity (up to two orders) are observed for the specimens with the content of the ferromagnetic alloy prior to the percolation threshold (27.38–35.63 at.%), which is due to the presence of poorly conducting islands and capacitance arising between these islands. The practically linear growth of conductivity is first of all due to the capacitance characteristics of the composite. After the percolation threshold for most films the dependences of the impedance module and conductivity on frequency weaken noticeably, and the capacitance contribution will not have significant effect on the conducting properties of composites.

In the microwave region the occurrence of most noticeable extrema of conductivity is also observed for the composites with the ferromagnetic alloy content of 27.38–35.63 at.% (Figure 2). This may be due to interference of two electromagnetic waves in phase opposition, reflected from the composite film and lavsan substrate

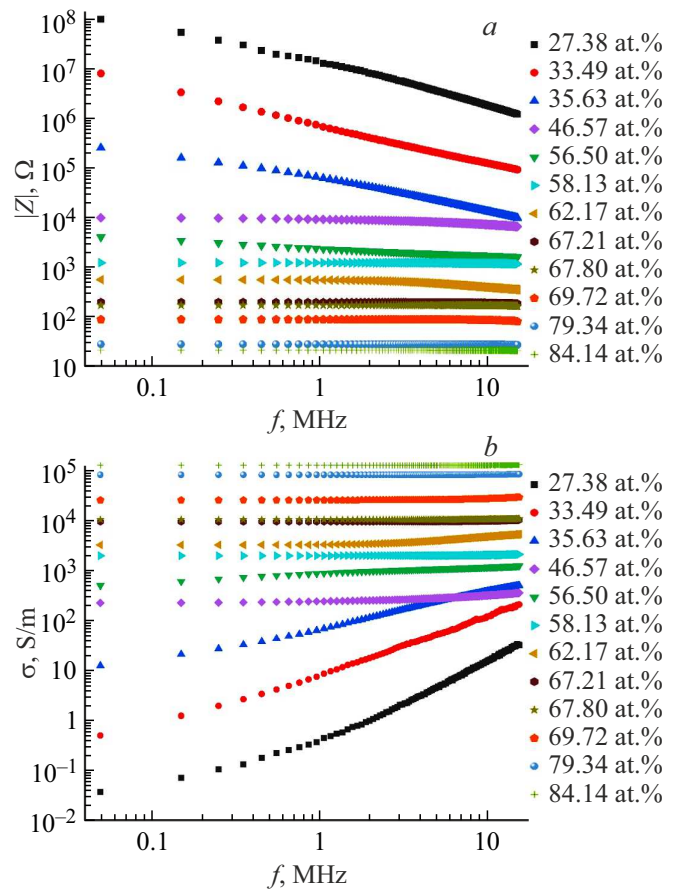


Figure 1. Dependences of impedance module Z and dynamic conductivity σ on the frequency in the range of 50 kHz–15 MHz.

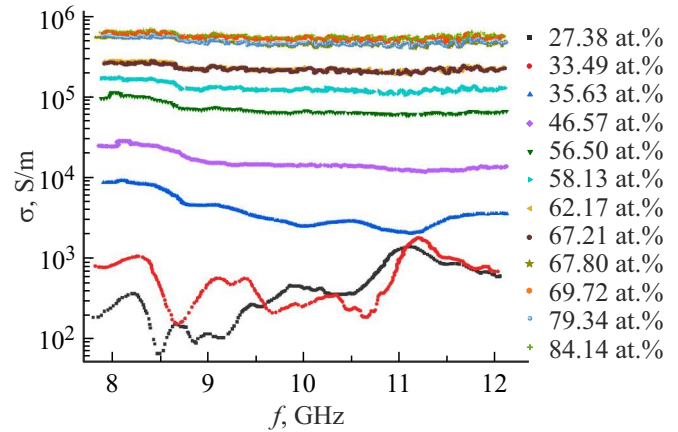


Figure 2. Dependences of dynamic conductivity σ on frequency in the range of 8–12 GHz.

when measuring the microwave reflection coefficient in the waveguide. As the content of the metal phase increases, the contribution of the reflected wave from the substrate is smoothed out, and the curves of dynamic microwave conductivity dependence on the frequency gradually level out.

Content of the ferromagnetic alloy, layer thickness, electrical resistance and specific conductivity of composite films $(\text{CoFeB})_x + (\text{SiO}_2)_{1-x}$

NN	Content of ferromagnetic alloy x , at.%	Layer thickness d , nm, thickness of substrate 0.02 mm	Electrical resistance r_0 , Ω	Specific conductivity σ_0 , S/m
1	27.38	560	$1.00 \cdot 10^8$	$2.68 \cdot 10^{-2}$
2	33.49	493	$1.76 \cdot 10^7$	$1.73 \cdot 10^{-1}$
3	35.63	583	$2.35 \cdot 10^5$	$1.09 \cdot 10^1$
4	46.57	697	$1.96 \cdot 10^4$	$1.10 \cdot 10^2$
5	56.50	774	$4.29 \cdot 10^3$	$4.52 \cdot 10^2$
6	58.13	635	$1.68 \cdot 10^3$	$1.41 \cdot 10^3$
7	62.17	849	$5.80 \cdot 10^2$	$3.04 \cdot 10^3$
8	67.21	825	$1.98 \cdot 10^2$	$9.18 \cdot 10^3$
9	67.80	862	$1.68 \cdot 10^2$	$1.04 \cdot 10^4$
10	69.72	675	$7.96 \cdot 10^1$	$2.79 \cdot 10^4$
11	79.34	670	$3.01 \cdot 10^1$	$7.44 \cdot 10^4$
12	84.14	565	$2.23 \cdot 10^1$	$1.19 \cdot 10^5$

Figure 3 shows the dependences of the ratio of dynamic conductivity to the static one for various waves of medium, high frequency and microwave ranges.

As one can see from Figure 3, at frequencies of 9 and 11 GHz the dynamic microwave conductivity prior to the percolation threshold exceeds the static one by more than 2–4 orders. The mechanisms of dynamic conductivity in the microwave range are controlled by the currents inside the granules of composite [11,13], providing the main contribution to reflection for the structures with the least content of metal phase. Static conductivity below

the percolation threshold is to a great extent determined by the dielectric phase of composites. In the region of the percolation threshold (46.57–56.50 at.%) the currents inside the granules, and dynamic microwave conductivity together with them increase significantly. This may explain a certain growth σ/σ_0 of experimental points in Figure 3. However, above the percolation threshold, the static conductivity is determined by the metal phase of composites, and its sharp growth results in gradual reduction of ratio σ/σ_0 . In logarithmic scale the given dependences are qualitatively described by the polynomial of fourth degree.

Without any contribution to the granular currents due to reflection of the microwave, the dynamic conductivity in the frequency range of 1–15 MHz is below the microwave conductivity, but it being higher than the static one prior to the percolation threshold is quite noticeable (up to 1–3 orders). According to Figure 3, the dynamic high frequency conductivity lessens with the increase of the ferromagnetic alloy content at an exponential rate. After the percolation threshold at $x > 56.50$ at.% the values of the dynamic and static conductivities are practically levelled out. At frequency of 50 kHz the ratio of σ/σ_0 prior to the percolation threshold is not more than 2–3.

4. Conclusion

In amorphous nanogranular composites the mechanisms of dynamic conductivity are controlled by currents inside the granules of the structure, which are most noticeable with the ferromagnetic alloy content prior to the percolation threshold and at the initial stage of the percolation processes. The dynamic microwave conductivity may exceed the static

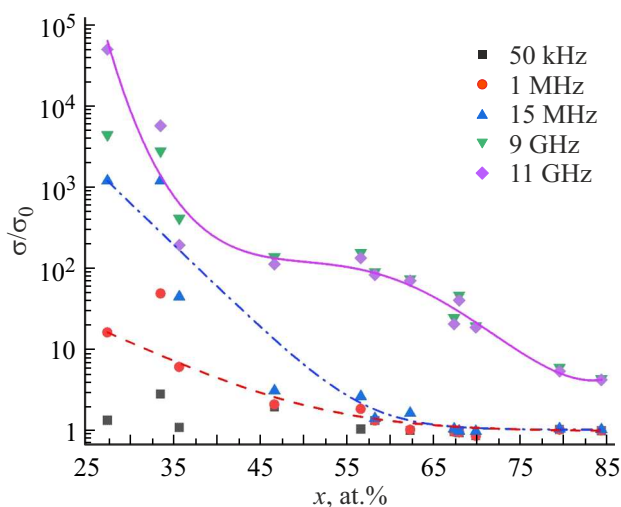


Figure 3. Dependences of the ratio of dynamic conductivity σ to static one σ_0 on the ferromagnetic alloy content for various frequencies.

one by more than 2–4 orders, and the high frequency one — up to 1–3 orders.

Funding

This study was supported by the Russian Science Foundation (grant No. 21-72-20048).

Conflict of interest

The authors declare no conflicts of interest.

References

- [1] A. Gerber, A. Milner, B. Groisman, M. Karpovsky, A. Gladkikh, A. Sulpice. *Phys. Rev. B* **55**, 10, 6446 (1997).
- [2] N.E. Kazantseva, A.T. Ponomarenko, V.G. Shevchenko, I.A. Chmutin, Yu.E. Kalinin, A.V. Sitnikov. *Fizika i khimiya obrabotki materialov* **1**, 5 (2002). (in Russian).
- [3] H. Gleiter. *Acta Mater.* **48**, 1, 1 (2000).
- [4] Yu.E. Kalinin, A.N. Remizov, A.V. Sitnikov. *Phys. Solid State* **46**, 11, 2146 (2004).
- [5] V.V. Klimov. *Phys. — Uspekhi* **66**, 3, 263 (2023).
- [6] T. Jungwirth, J. Sinova, A. Manchon, X. Marti, J. Wunderlich, C. Felser. *Nature Phys.* **14**, 3, 200 (2018).
- [7] K. Roy. *IEEE Trans. Nanotechnol.* **16**, 2, 333 (2017).
- [8] P.G. Baranov, A.M. Kalashnikova, V.I. Kozub, V.L. Korenev, Yu.G. Kusrayev, R.V. Pisarev, V.F. Sapega, I.A. Akimov, M. Bayer, A.V. Scherbakov, D.R. Yakovlev. *Phys. — Uspekhi* **62**, 8, 795 (2019).
- [9] A. Stupakiewicz, K. Szerenos, D. Afanasiev, A. Kirilyuk, A.V. Kimel. *Nature* **542**, 7639, 71 (2017).
- [10] A.I. Musorin, A.S. Shorokhov, A.A. Chezhegov, T.G. Baluyan, K.R. Safronov, A.V. Chetvertukhin, A.A. Grunin, A.A. Fedyanin. *Phys. — Uspekhi* **66**, 12, 1211 (2023).
- [11] I.V. Antonets, Ye.A. Golubev. *J. Phys. Chem. Solids* **184**, 111674 (2024).
- [12] I.V. Antonets, R.I. Korolev, L.N. Kotov. *FTT* **65**, 12, 2055 (2023). (in Russian).
- [13] I.V. Antonets, Ye.A. Golubev, V.I. Shcheglov. *Mater. Chem. Phys.* **290**, 126533 (2022).
- [14] I.V. Antonets, L.N. Kotov, Ye.A. Golubev. *Mater. Chem. Phys.* **240**, 122097 (2020).

Translated by M.Verenikina